# ANALYSIS OF PROPAGATION PROPERTIES OF STEP INDEX PLASTIC OPTICAL FIBERS AT NON-STATIONARY CONDITIONS

M. A. Losada (1), J. Mateo (1), L. Serena (1)
1: GTF, Aragón Institute of Engineering Research (i3A), Department of Electronic Engineering,
University of Zaragoza, María de Luna 1, 50018 Zaragoza, Spain.
Phone: +34 976 762360. Fax: +34 976 762111. E-mail: jmateo@unizar.es

***Abstract:*** *The aim of this paper is to characterize power propagation in step-index plastic optical fibers (SI-POFs) using short samples of the fibers. We measured the far field pattern (FFP) at the output of a short length of fiber (1.25 to 5m) changing the injection angle of a collimated light source. The FFPs obtained under these experimental conditions are very distinctive for each fiber type and thus, the diffusion characteristics derived from them can help to understand the optical power evolution throughout the fiber.*

## 1. Introduction

In a previous work [1], the diffusion and attenuation functions of three SI-POFs were estimated by fitting the profiles simulated using a model based on the generalized power flow equation [2] to those extracted from the FFPs measured with an overfilled launch. We found that, when diffusion was modeled as a function of the propagation angle, the predictions were in better agreement with the experimental data than when using the customary constant diffusion model. In fact, the estimated diffusion was a decreasing function of the angle, with the highest values for propagation near zero degrees. Later, simulations of the experiment proposed by Gambling [3] to estimate the coupling strength were compared to previous experimental estimates of this parameter providing further evidence suggesting a non-constant diffusion function [4]. In this paper we present the experimental FFPs of short SI-POFs captured for under-filled conditions obtained by direct launching of a He-Ne laser beam at different angles relative to the fiber axis. While these results still suggest that diffusion is a decreasing function of the propagation angle, the model is not able to reproduce precisely the quantitative behavior of the fiber at short lengths. In fact, we found that, after only 1.25m of light propagation, the measured far field profiles are considerably wider than those predicted by the model suggesting higher diffusion than was previously estimated for long fibers and over-filled launch.

Therefore, we propose a new approach to describe the fiber behavior that accounts for our experimental findings obtained with under-filled launch and short fiber lengths. The modeling of power propagation in POFs for non-stationary conditions is very important not only as the application scope of these fibers implies that its use is restricted to relatively short fiber lengths, but also for its strong relationship on bandwidth and losses [4]. In addition, we found that under the present experimental conditions the differences between the FFPs of different fibers are enhanced relative to our previous measurements of longer fibers under over-filled launch. Thus, this new approach devised for short fibers can help us to understand the variation with length of propagation properties characteristic of each fiber type.

This paper is organized as follows. In the first section we describe the experimental set-up and the procedure to obtain the radial profiles of the FFPs as a function of the launching angle. The model of fiber propagation based on the power flow equation is also outlined. In the second section, we present the results for three high numerical aperture (NA) step-index PMMA POFs from different manufacturers. In the discussion, we compare our experimental results to the previous model predictions. Their discrepancies will be the basis to describe diffusion in the first meters for each fiber, which is more distinctive for each fiber type, and that can better explain the variation of fiber bandwidth versus length.

## 2. Experiments and Models

In this section we present the experimental set-up and methodology used to capture the FFPs with a CCD camera and the results obtained for three PMMA fibers of 1mm diameter from different manufacturers: ESKA-PREMIER GH4001 (GH) from Mitsubishi, HFBR-RUS100 (HFB) from Agilent, and PGU-FB1000 (PGU) from Toray. The GH and PGU fibers have numerical aperture (NA) of 0.5 (corresponding to 19.5º inner critical angle) and 0.15dB/m of nominal attenuation. The HFB fiber has NA of 0.47 (18.5º inner critical angle) and 0.22dB/m of nominal attenuation.

### 2.1 Experimental methods

The experimental set-up, shown in Figure 1, is only briefly described as it is the same set-up thoroughly described in [1] and [4], except for the injection module. This module consists on a He-Ne laser beam of 635nm directly injected into the fiber input end, which is placed on the center of a rotary mount in order to vary the launching angle. The output end of the fiber is placed opposite a white screen and the reflected FFP image was registered using a 12 bit monochrome cooled camera QICAM FAST 1394. The maximum output angle is given by the spatial configuration of the set-up and in

this case was 37º (corresponding to an inner angle of 23.74º, above the critical angle for all fiber types). The experimental procedure was the following: we started with a 5m segment and measured the FFP varying the external launching angle from -32º to +32º in 1º steps. After taking the whole images series, we cut a 2.5m segment from the fiber input end and started again the characterization of the remaining 2.5m. Finally, a 1.25m segment was cut and the same process was repeated for the 1.25m segment. The fiber was always cut from the launching end, while the end facing the screen was fixed throughout the whole experiment. From the raw images the centroid was obtained and the radial profile was calculated by averaging the values of all the pixels at a given distance from it.

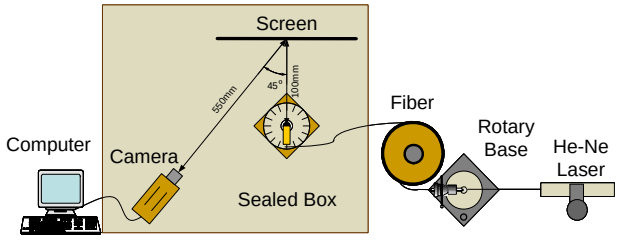


Figure 1: Experimental se-up to capture FFP images using a He-Ne laser at different launching angles.

We have also measured long fiber segments (100m and 75m) of the same fibers in order to do a further test of our proposals. The same procedure was followed but the launching angle was more coarsely sampled at four degrees steps.

In order to assess the impact of fiber end preparation, we have tested the repeatability of our measurements by preparing a 1.25m fiber and capturing the FFP for the whole angular scan three times. The results show only slight differences and we can conclude that the exact procedure of preparing the fiber and also its quality have little influence on the overall characteristics of the FFPs revealed in our measurements.

2.2 Model

We used the same model proposed in [1] based on a generalized power flow equation proposed by Gloge [2] where diffusion and attenuation are functions of the propagation angle:

$$\frac{\partial P(\theta,z)}{\partial z} = -\alpha(\theta)P(\theta,z) + \frac{1}{\theta}\frac{\partial}{\partial\theta}\left(\theta D(\theta)\frac{\partial P(\theta,z)}{\partial\theta}\right) \quad (1)$$

To predict our present measurements, this equation was solved introducing as the initial condition a narrow Gaussian function to model our launching distribution. Diffusion was modeled by the same sigmoid function of the squared inner angle proposed in [1], given by the following expression:

$$D(\theta) = D_0 + \frac{D_1}{1 + D_2 e^{\sigma_d^2\theta^2}}, \quad (2)$$

where $D_0$, $D_1$, $D_2$, and $\sigma_d$ are the free parameters of our model. The value of this diffusion function at small angles tends to $D_0 + D_1/(1+D_2)$, while for larger angles tends to $D_0$. The position and magnitude of the slope are governed jointly by $D_2$ and $\sigma_d$.

## 3. Results

We have used a 3D image representation to display all the profiles for the same fiber and length in a single plot. The images for the three fibers for 1.25m are shown in Figure 2 and for 5m in Figure 3. For the sake of simplicity, we do not present here the data for 2.5m because it shows similar characteristics than the others and does not add any new information. In each of the nine images of the figures, the horizontal coordinate is the launching angle. Thus, each column represents the radial profile obtained for the corresponding injection angle with higher values shown in lighter gray. The horizontal mirror images of the profiles, corresponding to negative output angles, are also shown for the sake of symmetry. In the images, the profiles are normalized so that they all have the same total power, which makes them independent of the angular attenuation function. Both the output angle and the launching angle are given as fiber inner-propagation angle in degrees. As the angular sampling of the radial profiles (0.13º) is much finer than the scanning steps of the launching angle (0.61º), a bicubic interpolation has been performed to get the same scale in both axis (0.25º). In the 3x3 graphs shown in Figures 2 and 3, each row shows the images for each fiber (GH, HFB, PGU from top to bottom, respectively).

The first column in both figures shows the experimental measurements that have the same qualitative pattern for all the fibers: a central square and two crossing diagonals starting from its corners. However, each fiber has a distinct quantitative behavior revealed by the different widths of both the square and the diagonals, and their relative magnitudes. This pattern indicates that there is a particular launching angle, which we will call the transition angle from now on, that marks the border between two different behaviors. For launching angles below the transition angle, power is quickly spread producing disk patterns, whose corresponding profiles have similar widths independently of the launching angle, illustrated by the central region in the images. For angles above the transition angle, however, the FFPs are ring patterns. Moreover, their peaks are located at an output angle equal to the launching angle, as shown by the diagonal lines at 45 degrees, which have a very narrow width. It can be seen that the HFB fiber has both the greater transition angle and the wider diagonals. The GH has larger transition angle than the PGU, but its diagonals are narrower. As we increase fiber length both the central part and the diagonals widen slightly (see Fig. 3).

The middle column of both figures shows the predictions with diffusion modeled for long fiber lengths [1], which are much narrower than our experimental results. The rightmost column shows the predictions obtained with our present proposal, which will be described in the next section.

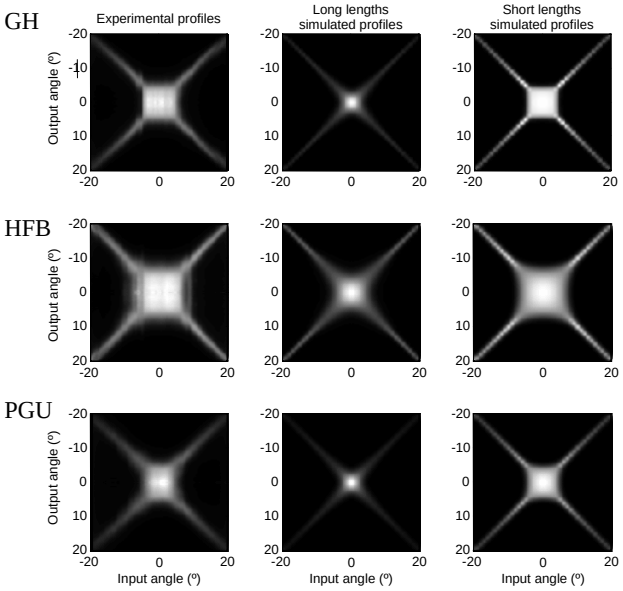


Figure 2: Profiles for 1.25m: experimental (left), simulated with diffusion for long (middle) and short (right) fibers.

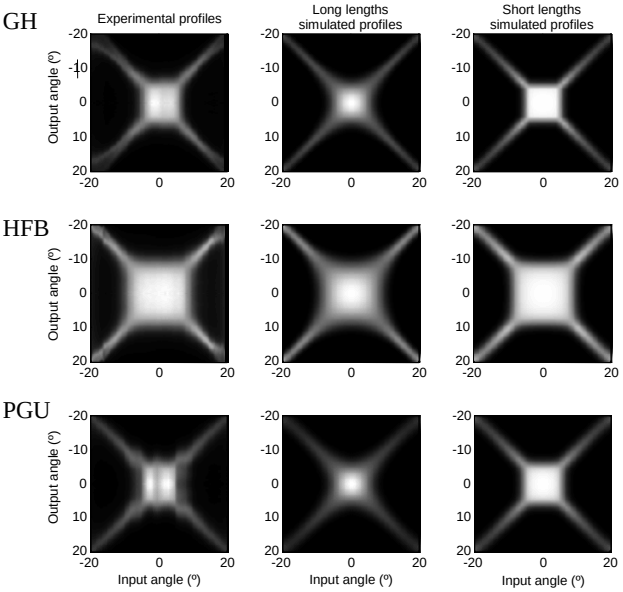


Figure 3: Profiles for 5m: experimental (left), simulated with diffusion for long (middle) and short (right) fibers.

## 4. Discussion

As we mentioned before, the profiles predicted by the model for long fibers, shown in the middle columns of the figures 2 and 3, are much narrower than those actually found. With increasing fiber length, model predictions become more similar to experimental results, although the predicted profiles for 5m are still narrower than the measured profiles. This comparison reveals that our diffusion functions previously estimated for long fibers cannot reproduce our present data. The differences suggest a very strong diffusion at lower angles to account for the observed widening of the profiles obtained for such a narrow source and in such a short distance. A different diffusion function with much higher values at low angles can account for this fast initial widening. Moreover, a small value at higher angles would explain the slow diffusion revealed by the long fiber lengths necessary to achieve the transition from ring to disk pattern when launching at high angles [4], and later to reach the steady state [1]. Thus, we varied the parameters to obtain new diffusion functions for each fiber type that reproduce better our measurements for short fiber lengths as show the images on the third column of the figures.

In Figure 4, the new diffusion functions are plotted for the three fibers tested along with those found for the same fiber types but using longer fibers [1] to allow their comparison. The figure shows that, as expected, the new diffusion functions have much higher values at a core of low angles, but that both functions are rather similar at higher angles. In the transition region, diffusion for short fibers decreases more steeply and at lower angles than the fall-off for the older diffusion functions. Figure 4 also permits to see the differences in diffusion between fibers, which can be quantified by the values of the parameters in Table 1, where both sets of parameters are given.

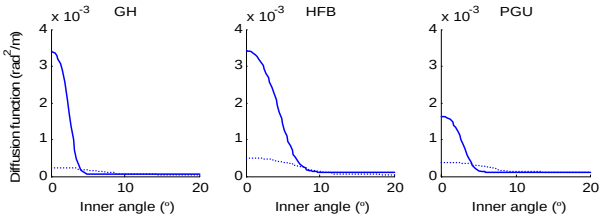


Figure 4: Diffusion functions obtained for short fibers (solid lines), along with those obtained for long fibers (dotted lines).

The diffusion functions previously obtained for long fibers are very similar for all fiber types, showing only slight differences at low angles. For short fibers, however, these differences at low angles are much more noticeable and each of the three fiber types can be distinguished by its particular diffusion function. Both GH and HFB fibers have a higher value at 0º than the PGU, but the HFB fiber diffusion is wider than the GH diffusion. The value at high angles, however, is very similar for all fibers in both conditions.

Table 1: Parameters for the diffusion function for short and long lengths.

| | | **GH** | **HFB** | **PGU** |
|---|---|---|---|---|
| Diffusion for short lengths | $D_0$ | $0.7\times10^{-4}$ | $1.0\times10^{-4}$ | $1.1\times10^{-4}$ |
| | $D_1$ | $40\times10^{-4}$ | $50\times10^{-4}$ | $20\times10^{-4}$ |
| | $D_2$ | 0.2 | 0.5 | 0.3 |
| | $\sigma_d$ | 32 | 15 | 25 |
| Diffusion for long lengths | $D_0$ | $0.6\times10^{-4}$ | $0.6\times10^{-4}$ | $1.5\times10^{-4}$ |
| | $D_1$ | $2.3\times10^{-4}$ | $6.5\times10^{-4}$ | $3.0\times10^{-4}$ |
| | $D_2$ | 0.32 | 0.5 | 0.2 |
| | $\sigma_d$ | 11.7 | 9.6 | 12.6 |

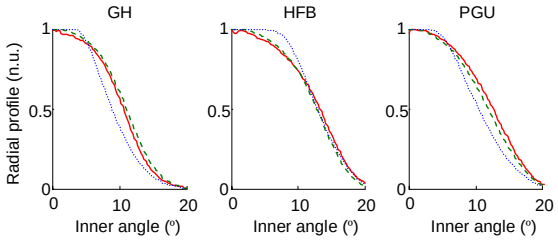


Figure 5: Comparison of our present data (solid line) for 75m to predicted profiles using both diffusion models, for short lengths (dotted line) and for long lengths (dashed line).

The question remains now if the model found for short fibers holds as well for longer fibers. A comparison between the FFP profiles predicted with the old and new diffusion functions and our present measurements for 75m launching at 0º is shown in Figure 5. The predictions of the present model display a very different shape to that of the measured profiles, mainly in the central region which, in the predicted profiles, agglutinates more power than the center of the actual measurements. To obtain the fast initial power spread, the diffusion function has to be very high at lower angles and thus, even after propagation through a long fiber segment, power is still confined to this central region. However, the predictions obtained for the diffusion functions fitted to data for longer fiber lengths are in a very good agreement with our current data even though the later were obtained injecting with a collimated laser instead of a semiconductor laser.

Our findings suggest that it is not possible to find a single diffusion function to characterize a fiber type for all fiber lengths. Thus, we conclude that a more accurate model of fiber propagation includes a diffusion function that changes with length with values at low angles much higher for shorter than for longer fibers, while at high angles the values are lower and practically constant with length. This dependence of diffusion with length implies that the power flow equation is a length-variant coefficient equation. We suggest that the ultimate physical cause could be the stochastic behavior of diffusion whose averaged estimate is smoother than the responses of the individual concatenated short fibers.

As a result of the changes in diffusion with length, power launched into lower angles is rapidly spread to a cone of angles whose radius depends more on the fiber type than on the source distribution. After these first meters, the power keeps confined to this region throughout propagation but there is some spread into higher angles revealed by the slow widening of the profiles with length. This slow spread is due to the low value of the diffusion function at long lengths. When launching at higher angles, where the value of diffusion is always very low, the FFPs have a ring shape which is hardly changed throughout propagation except for the strong attenuation that renders them hardly measurable for long fibers. In the middle angular region, we have an intermediate behavior and power is transferred to lower angles, and, after a considerable length, it is possible to reach the steady state distribution whose shape is mainly determined by the angular attenuation.

Therefore, we can conclude that power diffusion at the first fiber meters determines the main characteristics of its angular power distribution through most of the fiber with only minor changes introduced by slow diffusion and angular attenuation. In fact, it is not unreasonable to think that diffusion for large fibers could be modeled by an initial pattern given by the strong diffusion found for short fibers and specific for each fiber type, followed by a small constant diffusion.

Moreover, we suggest that this behavior must have a strong impact to pulse widening and consequently, to fiber dispersion and bandwidth. All power confined to the lower angles will follow a similar trajectory as there is only a minor spread toward higher angles, which implies that they will have the same overall delay and thus, will hardly contribute to temporal pulse broadening. Higher angles will propagate slowly and more or less independently increasing pulse width as a function of fiber length.

## 5. Conclusions

Our results for short fibers suggest that diffusion can be modeled by a function similar to that for longer fibers, but with higher values at low angles. This diffusion function cannot reproduce precisely profiles for longer fibers, suggesting that diffusion is a length-dependent function. However, diffusion in the first meters, which depends strongly on fiber type, determines power distribution characteristics through most of the fiber. Thus, we propose that short fiber diffusion can be used to characterize the fiber behavior and may have a strong impact in propagation properties such as bandwidth and losses.

## 6. Acknowledgement

This work was supported by the Spanish Government under grant TEC2006-13273-C03-02.

## 7. References

[1] J. Mateo, M.A. Losada, I. Garcés, J. Zubia, "Global characterization of optical power propagation in step-index plastic optical fibers," Optics Express 14, 9028-9035 (2006).

[2] D. Gloge, "Optical Power Flow in Multimode Fibers," B.S.T.J. 51, 1767-1783 (1972).

[3] W.A. Gambling, D.N. Payne, and H. Matsumura, "Mode Conversion Coefficients in Optical Fibers," Appl. Opt. 15, 1538-1542 (1975).

[4] M.A. Losada, J. Mateo, I. Garcés, J. Zubia, "Estimation of the attenuation and diffusion functions in plastic optical fibers from experimental far field patterns" in Proceedings of the 15th International Plastic Optical Fibers Conference (2006) , pp. 336-341.

[5] P. Heredia, J. Mateo, M.A. Losada, "Transmission capabilities of large core GI-POF based on BER measurements" in Proceedings of the 16th International Plastic Optical Fibers Conference, (2007), in press.